THE JOURNAL OF PHYSICAL CHEMISTRY A LETTERS

2006, *110,* 12355−12359
Published on Web 10/21/2006

Two-Dimensional Fluorescence (Excitation/Emission) Spectroscopy as a Probe of Complex Chemical Environments

Neil J. Reilly, Timothy W. Schmidt,* and Scott H. Kable*

School of Chemistry, University of Sydney, Sydney, NSW 2006, Australia

Received: July 13, 2006; In Final Form: September 14, 2006

We report a new application of fluorescence spectroscopy for the identification and characterization of chemical species in complex environments. Simultaneous collection of a dispersed fluorescence spectrum for every step of the laser wavelength results in a two-dimensional spectrum of emission versus excitation wavelengths. This two-dimensional fluorescence (2DF) spectrum yields quick and intuitive assignments of a multitude of peaks in the separate fluorescence excitation and dispersed fluorescence spectra as belonging to the same species. We demonstrate the technique with the measurement of 2DF spectra of a discharge of dilute benzene into a supersonic free jet. A multitude of rovibronic bands due to the C_2 Swan and C_3 comet bands are immediately apparent and even unreported bands can be assigned intuitively. Custom software filters are employed to enhance or reject emission from one or the other carrier to obtain excitation spectra arising from purely one carrier, or even a specific spectral component of a single carrier. The very characteristic 2DF fingerprints of C_2 and C_3 permit identification of another unidentified species in the discharge that absorbs at 476 nm, coincident with one of the diffuse interstellar bands.

Introduction

Laser induced fluorescence (LIF) excitation spectroscopy has become one of the signature spectroscopic techniques of the laser age. Its sensitivity and high resolution have ensured that is used ubiquitously in a very wide range of applications, including combustion diagnostics, detection of trace atmospheric species, fluorescence microscopy and reaction dynamics.[1−4] Dispersed fluorescence (DF) spectroscopy is likewise a very powerful technique for identification of the spectroscopic carrier, and also for spectroscopic measurement of ground-state vibrational frequencies, although its application is perhaps not as widespread.[5]

Complex chemical environments lessen the utility of most spectroscopic techniques because many species can absorb and emit at similar wavelengths. When the chemical environment contains unknown species, unravelling the absorption or emission features that belong to separate molecular species becomes even more challenging. Higher dimensional spectroscopic techniques can be employed to yield much higher quality information when the spectrum in one dimension is complex. For example, in NMR spectroscopy, 2D techniques such as NOESY and COSY reveal spatial correlations between protons on the same molecule. There are also optical analogues of 2D NMR spectroscopy, for example, 2D IR photon echo spectroscopy. The two dimensions need not be both in time. For example, step-scan FTIR techniques are also 2D techniques, where one dimension is wavelength and the other time; fluorescence lifetime scanning provides similar information in the ultraviolet. All of these examples (which is not at all a comprehensive list) provide excellent examples of utilizing the correlation between two dimensions to provide a deeper understanding of a particular phenomenon than scans in each single dimension could provide.

In this paper, we report the measurement of two-dimensional fluorescence (2DF) excitation/emission spectroscopy of a complex chemical environment—a supersonically cooled hydrocarbon discharge. The objective of this paper is to show that the 2DF spectrum provides a more immediate and intuitive connection between correlated peaks in the excitation and emission spectra than do the individual one-dimensional spectra. If one part of the 2DF spectrum is understood, then many unknown, previously overlapping features in the 1D excitation (exc) and/or emission (em) spectra can be identified simply. Common signatures of known and unknown species can be grouped together, which enhances the identification of the unknown features and/or chemical species by spectroscopic means.

We demonstrate the power of this technique by reporting the 2DF spectrum in the wavelength range $\lambda_{exc} = 455-480$ nm and $\lambda_{em} = 410-580$ nm) of the products of a benzene/Ar discharge, expanded in a supersonic free jet expansion. The conventional 1D excitation and emission spectra are complex—dominated by the very strong C_2 Swan and C_3 comet bands. There are also many underlying, weak rovibronic transitions of these carriers that contaminate all the 1D spectra, making positive identification of weak spectroscopic carriers in the discharge very difficult. We also demonstrate that the 2DF spectrum provides a much more intuitive picture of the weaker C_2 and C_3 features than the independent 1D spectra. Many weak transitions can be quickly attributed to C_2 and C_3, leaving a much cleaner palate to begin spectroscopic identification of

---

* Corresponding authors. E-mail: s.kable@chem.usyd.edu.au (S.H.K.); t.schmidt@chem.usyd.edu.au (T.W.S.).

10.1021/jp064411z CCC: $33.50

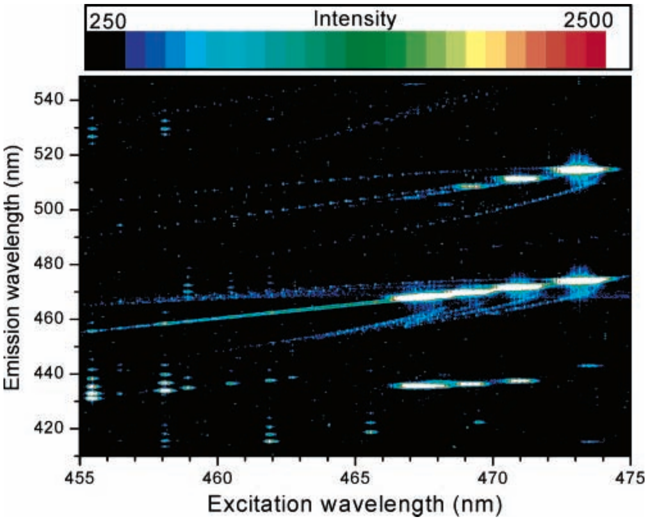

Figure 1. 2D excitation−emission spectrum of a benzene−Ar discharge. The C_2 bands form the "comet-like" features with very intense bandheads and prominent "tails" caused by P and R rotational branches. The C_3 fingerprint is the set of tight spots, about 2 nm apart on the λ_{em} axis, degraded to the red. The oblique line where $\lambda_{exc} = \lambda_{em}$ is formed by fluorescence that is resonant with the laser excitation.

unknown species. The first unknown species identified by us using this method has an origin absorption feature at 476 nm, which happens to coincide with one of the stronger absorption features comprising the diffuse interstellar bands (DIBs).

Experimental Section

Benzene (~0.1%) in Ar is expanded into a vacuum chamber via a pulsed nozzle. Attached to the nozzle is a pair of electrodes, across which a pulsed electrical potential of up to 2 kV is applied. The electrical pulse (50 μs) is timed to occur in the middle of the gas pulse (200 μs). The discharge fragments the benzene and a wealth of recombination chemistry occurs, depending on the timing of the electrical pulse and the pressure of the benzene and Ar. An excimer pumped dye laser crosses the free jet expansion about 2 cm downstream, immediately after the voltage is switched off, which minimizes interference from discharge afterglow. In this work the dye laser is tuned from 445 to 480 nm (C460 dye).

Fluorescence emission is collected via *f*/1 optics and imaged onto the slits of a spectrograph. The emission is dispersed across the 2D CCD array as a series of images of the entrance slit dispersed in wavelength. The 2D array is detected by an intensified CCD camera. The camera hardware sums the slit image for each wavelength over 5−200 laser shots and then returns a 1D array of intensity versus emission wavelength to the computer. A complete DF spectrum is therefore collected and integrated for every laser step or series of steps. The data are collected on a PC, accumulated into a 2D excitation versus emission wavelength array, which is then analyzed using custom and free image analysis software. Once a new feature in the spectrum has been identified, higher resolution 1-D DF spectra are obtained using a 0.75 m scanning spectrometer.

Results and Discussion

Overview of 2DF Spectrum. A 2DF spectrum of the benzene-Ar discharge is shown in Figure 1. The laser excitation wavelength (λ_{exc}) was scanned from 455 to 475 nm, which is shown along the abscissa. The emission wavelength (λ_{em}) is plotted as the ordinate. Fluorescence intensity is represented by a 25 color map, with a color scale above the figure. There is a wealth of structure in both dimensions and a very wide dynamic range of fluorescence intensity. Each pixel is the sum of intensity of each CCD element × 60 rows of the CCD × 200 laser shots. The total intensity in the spectrum therefore has a very wide dynamic range, which in Figure 1 ranges from 0 to 160 000 for the strongest band. The spectrum shown has been truncated to 250−2500; very intense features beyond this scale are shown in white, and the noise level (<250) is shown in black.

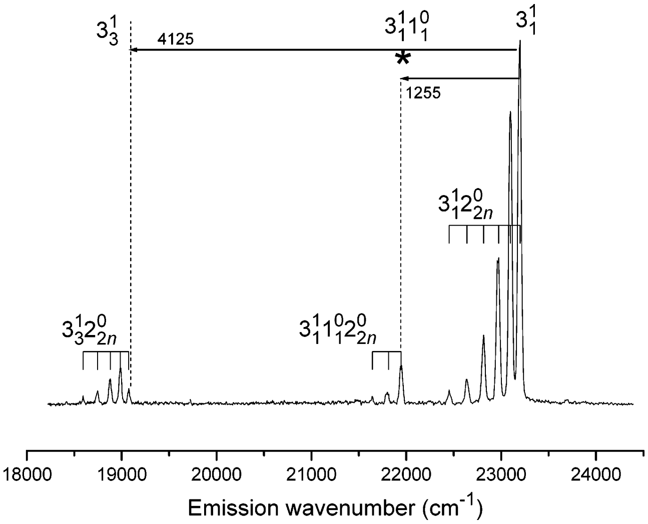

Figure 2. Dispersed fluorescence spectrum extracted from the 2DF spectrum in Figure 1 at $\lambda_{exc} = 455.5$ nm. The structure is assigned as C_3 $\tilde{A} \rightarrow \tilde{X}$ emission following excitation of the 3^1 level via the $1^0_1 3^1_1$ transition. The excitation position is marked with an asterisk.

Each feature in the spectrum can be represented as a (λ_{exc}, λ_{em}) coordinate. A bright band appears in the spectrum where $\lambda_{exc} = \lambda_{em}$. Fluorescence features that lie along this line are resonant with the laser excitation wavelength. For example, the very strong feature at (λ_{exc}, λ_{em}) = (473, 473) nm is C_2 (1→0) resonance fluorescence. Features that lie below the resonance fluorescence line have $\lambda_{em} < \lambda_{exc}$ and therefore clearly indicate that the excitation feature is a hot band.

Many of the features in Figure 1 are due to well-known C_2 and C_3 transitions.[6−10] We use these well-known transitions to demonstrate some of the advantages that 2DF offers over independent 1D excitation and emission spectra. Then, having a more secure understanding of the 2DF spectrum, we point out some unidentified fluorescence that does not belong to C_2 or C_3.

C_3 Features. A clear fluorescence fingerprint, of which the peaks near (455.5, 431.5) are representative, is observed throughout the 2DF spectrum in Figure 1. The fingerprint is characterized by several peaks with slightly increasing spacing, which is usually degraded to the red in the λ_{em} coordinate. A conventional dispersed fluorescence spectrum, extracted from the 2DF spectrum by taking a vertical slice through the spectrum at $\lambda_{exc} = 455.5$ nm, and converted to wavenumber units, is shown in Figure 2. The spectrum is the C_3 $\tilde{A}(^1\Pi_u) \rightarrow \tilde{X}(^1\Sigma_g^+)$ 3^1 emission spectrum, which is one of the "comet bands" (also referred to as Swings bands). The most intense feature, displaced about 1255 cm^{-1} to the blue of the excitation position, is the 3^1_1 transition, reported previously by Izuha and Yamanouchi.[11] The emission spectrum is assigned simply as 3^1 emission and shows progressions in ν_1'', $2\nu_2''$ and $2\nu_3''$—the symmetric stretch, bend and asymmetric stretch of ground-state C_3 respectively.[11]

These very characteristic C_3 fingerprints are seen throughout the 2DF spectrum. Many of these transitions have not been reported previously, but it is not our intent to proffer assignments here. For the purposes of this report their identity as C_3 comet band emission is unmistakable.

C_2 Features. Very strong Swan band emission dominates the 2DF spectrum in Figure 1. As assigned previously, the resonance fluorescence at (473, 473) is the $1\rightarrow0$ emission band. Peaks corresponding to the (1,1) emission are also strong at (473, 514). The (2, 1), (3, 2), and (4, 3) hot-band sequences are also obvious in resonance fluorescence, between (473, 473) and (467, 467). These hot bands also form sequence-like structure starting from (471, 437). The assignment of these excitation transitions as hot bands is secure by this observation of blue-shifted fluorescence, which is trivial for C_2, but vital information for unassigned LIF bands. Another red-shifted group of bands forms a sequence in emission, starting at the (473, 514) peak; these are the ($n \rightarrow n$) sequences near the C_2 electronic origin.

There are also two much weaker features belonging to C_2 located at (473.6, 442.6) and (473.6, 415.0) nm. In the 1-D LIF spectrum, which is the vertically integrated 2DF spectrum, these features are buried beneath the strong ($1\leftarrow0$) band. They are not associated with the strong bands but are assigned as the C_2 ($9\rightarrow8$) and ($9\rightarrow7$) transitions, which arise following excitation of the $9\leftarrow9$ sequence, which is buried beneath the strong $1\leftarrow0$ transition. Clearly, C_2 is formed with extensive vibrational excitation in the discharge, which is incompletely cooled in the expansion.

Several flagellum-like features start at each of the principle Swan band peaks and decay behind the main peaks to the blue on the λ_{exc} axis. These are the $\Delta J = \pm1$ rotational transitions of each main vibrational band. These are directly related to, and a beautiful spectroscopic depiction of, the well-known Fortrat parabolas. The emission on each flagellum that follows diagonally behind the main features arises from both R-branch and P-branch excitation followed by the same transition in emission. The red-shifted flagellum on the λ_{em} axis arises from excitation of an *R*-branch transition with subsequent P-branch emission, and the reverse for the blue-shifted flagellum. (Q-branch transitions are also allowed in this biradical, triplet−triplet spectrum; however, the line strengths reduce rapidly for higher *J*.)[12]

The rotational branches extend throughout the whole range of the LIF excitation spectrum and show clearly why C_2 emission contaminates all emission spectra in this spectral region. Individual rotational transitions can be seen clearly in the flagella of the sequence bands near $\lambda_{em} = 500$ nm with a spacing that increases for higher *J*. The well-resolved features in the flagella correspond to $J > 50$ and again demonstrate that cooling is incomplete in the expansion. It should be pointed out, though, that the intensity of these features is 3 orders of magnitude weaker than the bandheads, which demonstrates the dynamic range in the spectrum.

Further rotational branch features are also evident near $\lambda_{em} = 530$ nm, which arise from the C_2 $1\rightarrow2$ band, the rotational origin of which is off the scale to the top right. The signature of these flagella as belonging to C_2, despite the main bandhead not appearing in the spectrum, is unambiguous.

In this 2DF spectrum, the multitude of rovibronic transitions belonging to C_2 can be assigned clearly and intuitively, even though in either of the conventional excitation or emission spectra they would be strongly overlapping and require accurate spectral simulation to deconvolve from one another, and from bands belonging to other carriers.

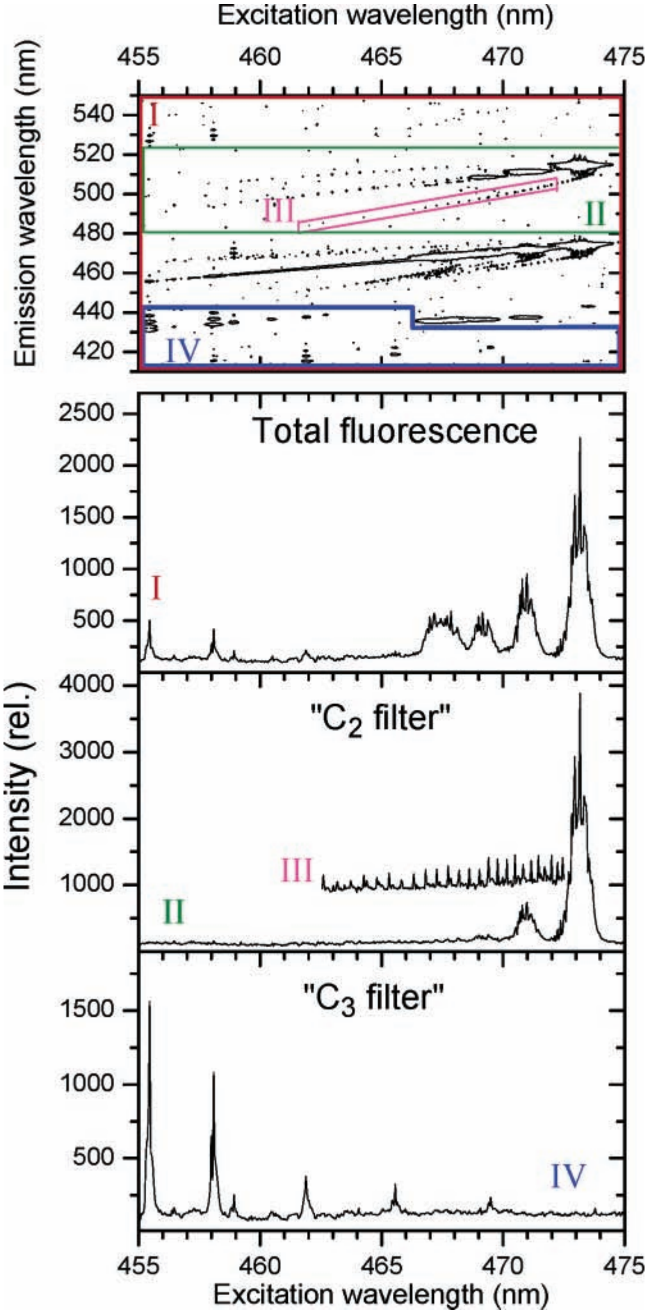

Figure 3. Single contour map of the 2DF spectrum of benzene−Ar discharge (top). The three spectra below are excitation spectra taken using four different software filters: (I) whole fluorescence excitation spectrum; (II) band-pass filter to enhance main C_2 spectral features; (III) custom filter to enhance the P-branch transitions in the C_2 $\upsilon = 1\leftarrow0$ transition; (IV) notch filter to enhance C_3 transitions.

Manipulating the 2DF Spectrum. The 2DF spectrum can be sliced to produce many emission spectra, an example of which was used in the C_3 analysis above and shown in Figure 2. The 2DF spectrum can also be sliced to produce fluorescence excitation spectra with a custom filter that can enhance particular absorption features, or remove interfering features. Figure 3 shows the same 2DF spectrum as Figure 1, but as a single contour plot corresponding to an intensity of 600. The spectrum (I) in Figure 3 corresponds to a conventional LIF excitation spectrum, monitoring total fluorescence. The C_2 and C_3 features are apparent, but many weaker overlapping transitions are obscured.

The green box marked (II) employs a simple filter that acts like an optical band-pass filter. This filter eliminates C_3 from the spectrum by choosing a region that has very little C_3

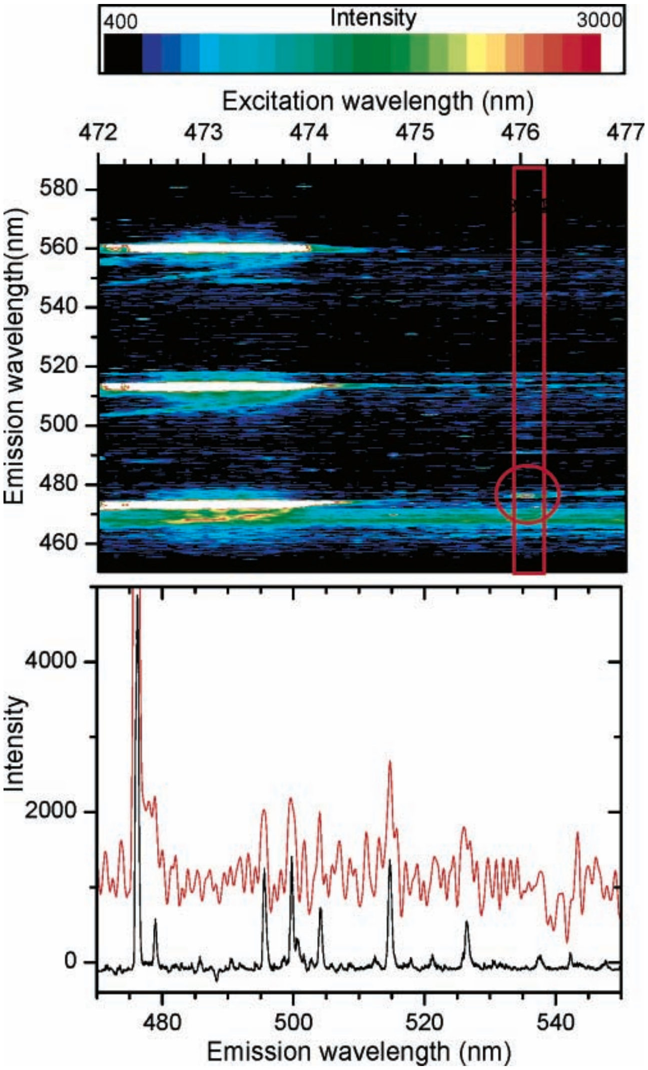

Figure 4. 2DF spectrum of jet-cooled benzene−Ar discharge (top). The dispersed fluorescence spectrum of a weak feature in the excitation spectrum at 476 nm is shown below. The red spectrum is the 476 nm slice of the 2DF spectrum. The black spectrum is a DF spectrum taken with a high-resolution scanning monochromator after optimizing the production of the unknown carrier.

emission, but strong C_2 emission. Specific spectral features of the C_2 emission can also be enhanced, as illustrated by the custom-filter (III). The ensuing excitation spectrum (also III) shows exclusively the C_2 ($\upsilon = 1 \leftarrow 0$) P-branch in absorption, obtained by detecting ($1 \rightarrow 1$) *R* branch emission. This filter has a constant width, but the central wavelength changes parabolically, following the Fortrat parabola, as the excitation wavelength is scanned. The rotational structure, which was completely obscured in spectra (I) and (II), is well-defined.

The blue box marked (IV) employs a different type of filter. The very strong C_2 ($2 \rightarrow 0$), ($3 \rightarrow 1$) and ($4 \rightarrow 2$) transitions emit at the same wavelength as the strongest C_3 features. A custom "notch" filter, which changes width in a stepwise fashion at $\lambda_{\mathrm{exc}} = 466.25$ nm, was employed to allow 440 nm emission around the C_3 features but to suppress it around the C_2 features. The excitation spectrum (IV) now shows only transitions due to C_3.

Unidentified Carrier Bands. The majority of 2DF structure in this spectral region can be identified as belonging to C_2 and C_3. However, there is some weak structure, slightly to the red of the region in Figure 1, that cannot be assigned to either of these carriers. Figure 4 (top) shows a 2DF spectrum covering $\lambda_{\mathrm{exc}} = 472-477$ nm and $\lambda_{\mathrm{em}} = 460-580$ nm. The three very intense features are again C_2 Swan emission, as identified in Figure 1. One resonance fluorescence feature has been circled at (476, 476) nm. This feature does not belong to C_2 or C_3. The red box highlights some of the emission structure that accompanies it; all features are extremely weak with an intensity more than 1000× weaker than the main C_2 and C_3 features. The red DF spectrum in Figure 4 shows a one pixel DF slice of the 2DF spectrum with $\lambda_{\mathrm{exc}} = 476$ nm utilizing a 5 point Fourier smoothing function. Although weak, there is clear dispersed fluorescence structure.

The discharge conditions were optimized to enhance the 476 nm feature and a high resolution dispersed fluorescence spectrum of the 476 nm feature was obtained using a conventional scanning monochromator. This spectrum is shown overlaid over the 2DF slice. The spectra are clearly of the same carrier. The molecule in question appears to be polyatomic hydrocarbon with several active vibrational modes.

We are currently attempting to identify the carrier of these unknown spectral features. Using custom filters, as described above, we have measured several other absorption and emission transitions of this carrier and aim to report on this in a later publication. The special interest in the carrier of these spectral features is that one of the stronger diffuse interstellar bands (DIBs) also occurs at 476 nm. The width of the observed transition is significantly narrower that the measured DIB. This might be because the observed laboratory carrier is different to the interstellar carrier, or that the interstellar spectrum is broadened by a mechanism not present under laboratory conditions. However, it is intriguing to note that this is the second report of an unknown carrier produced in a benzene discharge that absorbs at a wavelength coincident with a strong DIB.[13,14]

In summary, we report two-dimensional (λ_{exc}, λ_{em}) fluorescence spectroscopy of a complex chemical environment. Although the spectral features are strongly overlapping in the conventional excitation and emission spectra, the 2DF spectrum can be used to simply identify common carriers. We demonstrate that custom software filters can be applied to extract excitation spectra of individual species, and individual spectral features of a single carrier. The simple grouping of common carriers using this technique has allowed us to identify a spectral signature of an unknown molecule in the benzene discharge. The molecule is clearly polyatomic, and has a strong vertical transition at 476 nm, which coincides with one of the stronger DIBs.

Acknowledgment. This research was supported by a grant from the Australian Research Council (DP0665831). N.J.R. acknowledges the support of a Gritton Ph.D. stipend from the University of Sydney. We also gratefully acknowledge the support of Dr Klaas Nauta for fruitful discussion about this work.

References and Notes

(1) Kohsehoinghaus, K. *Prog. Energy Combust. Sci.* **1994**, *20*, 203.

(2) Stevens, P. S.; Mather, J. H.; Brune, W. H. *J. Geophys. Res.—Atmos.* **1994**, *99*, 3543.

(3) Weiss, S. *Science* **1999**, *283*, 1676.

(4) For example, see: Yin, H. M.; Kable, S. H.; Zhang, X.; Bowman, J. M. *Science* **2006**, *311*, 1443.

(5) But see: Nakajima, M. Yoneda, Y.; Toyoshima, H.; Sumiyoshi, Y.; Endo, Y. *J. Mol. Spectrosc.* **2005**, *232*, 255.

(6) Wollaston, W. *Trans. R. Soc. London* **1802**, *11*, 365.

(7) Swan, W. *Trans. R. Soc. Edinburgh* **1857**, *21*, 411.

(8) Johnson, R. C. *Philos. Trans. R. Soc. London A* **1927**, *226*, 157.

(9) Swings, P. *Rev. Mod. Phys.* **1942**, *14*, 190.

(10) Douglas, A. E. *Astrophys. J.* **1951**, *114*, 466.

(11) Izuha, M.; Yamanouchi, K. *J. Chem. Phys.* **1998**, *109*, 1810.

(12) Herzberg, G. *Spectra of Diatomic Molecules*; D. Van Nostrand Co.: New York, 1950.

(13) Ball, C. D.; McCarthy, M. C.; Thaddeus, P. *Astrophys. J.* **2000**, *529*, L61.

(14) Araki, M.; Linnartz, H.; Kolek, P.; Ding, H.; Boguslavskiy, A. E.; Denisov, A.; Schmidt, T. W.; Motylewski, T.; Cias, P.; Maier, J. P. *Astrophys. J.* **2004**, *616*, 1301.